INFECTION AND IMMUNITY, July 2002, p. 3673–3680 Vol. 70, No. 7
0019-9567/02/$04.00+0 DOI: 10.1128/IAI.70.7.3673–3680.2002

Strain-Dependent Induction of Enterocyte Apoptosis by *Giardia lamblia* Disrupts Epithelial Barrier Function in a Caspase-3-Dependent Manner

Alex C. Chin,[1] Desiree A. Teoh,[1] Kevin G.-E. Scott,[1] Jonathon B. Meddings,[2] Wallace K. Macnaughton,[3,4] and Andre G. Buret[1,4]*

Departments of Biological Sciences,[1] Medicine,[2] and Physiology and Biophysics,[3] and Mucosal Inflammation Research Group,[4] University of Calgary, Calgary, Alberta, Canada T2N 1N4

Received 14 December 2001/Returned for modification 28 January 2002/Accepted 21 March 2002

We recently demonstrated that *Giardia lamblia* rearranges cytoskeletal proteins and reduces transepithelial electrical resistance. The effect of *G. lamblia* on enterocyte apoptosis is unknown, and a possible link between microbially induced enterocyte apoptosis and altered epithelial permeability has yet to be established. The aim of this study was to assess whether *G. lamblia* induces enterocyte apoptosis in duodenal epithelial monolayers and whether this effect increases epithelial permeability. Monolayers of nontransformed human duodenal epithelial cells were incubated with sonicated or live *G. lamblia* trophozoites (NF, S2, WB, or PB strains) for 8, 24, and 48 h. Cell cultures were assessed for apoptosis by Hoechst fluorescence staining, enzyme-linked immunosorbent assay for apoptotic nucleosomes, and electron microscopy. In separate experiments, monolayers were pretreated with or without 120 μM caspase-3 inhibitor (Z-DEVD-FMK) for 1 h and were assessed for production of apoptotic nucleosomes, tight junctional integrity (with fluorescent ZO-1 staining followed by confocal laser microscopy), and transepithelial permeability for fluorescein isothiocyanate-dextran. *G. lamblia* strains NF and S2, but not strains WB or PB, induced enterocyte apoptosis within the monolayers, and this effect was inhibited by Z-DEVD-FMK pretreatment. Using the *G. lamblia* NF isolate, additional experiments investigated the possible link between enterocyte apoptosis and altered epithelial permeability. *G. lamblia* NF disrupted tight junctional ZO-1 and increased epithelial permeability, but these effects were also prevented by pretreatment with the caspase-3 inhibitor. These findings indicate that strain-dependent induction of enterocyte apoptosis may contribute to the pathogenesis of giardiasis. This effect is responsible for a loss of epithelial barrier function by disrupting tight junctional ZO-1 and increasing permeability in a caspase-3-dependent manner.

Giardia lamblia is the most frequently identified etiologic agent of waterborne disease worldwide (38). Giardiasis is characterized by acute or chronic diarrhea, dehydration, abdominal discomfort, and weight loss (18). During infection, *Giardia* trophozoites colonize the proximal small intestine and adhere to the apical surface of the enterocyte (18). This close association between the parasite and the small intestinal epithelium initiates a succession of pathophysiological processes, leading to a diffuse shortening of the epithelial microvilli (12, 54). The reduction of small intestinal absorptive surface area causes disaccharidase deficiencies and malabsorption of nutrients, water, and electrolytes (11, 12). The mechanisms responsible for abnormalities in epithelial structure and function during giardiasis remain poorly understood. Recent reports indicate that both host and parasitic products are involved in the pathogenesis of giardiasis. Indeed, the diffuse shortening of brush border microvilli and the associated disaccharidase deficiencies appear to be modulated by T lymphocytes (51). In contrast, live *G. lamblia* trophozoites, parasitic extracts, or supernatants obtained from live parasitic cultures directly induce calcium-dependent cytoskeletal F-actin and α-actinin changes in human colonic carcinoma monolayers and in nontransformed duodenal epithelial cells (55). Moreover, the cytoskeletal reorganization induced by *G. lamblia* is associated with a reduction in transepithelial electrical resistance across human duodenal epithelial cell monolayers (55). Another study reported that colonization with *G. lamblia* in Mongolian gerbils increased macromolecular uptake in the jejunum during the acute phase of the infection but not during the parasite clearance stage (26). Epithelial tight junctional complexes consist of proteins belonging to the zonula-occludens (ZO), claudin, occludin, and cingulin families (2, 23). ZO-1 is a 220-kDa peripheral membrane protein that interacts with tight junctional occludin at its N terminus and with cytoskeletal F-actin at its C terminus (2, 17). The intermediary role between the cytoskeleton and the tight junction played by ZO-1 underscores its importance in regulating paracellular permeability. *Vibrio cholerae* increases intestinal permeability by releasing a ZO enterotoxin (Zot) which binds Zot receptors expressed on mature small intestinal absorptive cells. This in turn causes the eventual displacement of tight junctional proteins, including ZO-1 (19, 20). In addition to the direct alteration of tight junctions by microbial factors, it was recently proposed that apoptosis may be another possible cause of increased intestinal permeability. Enhanced apoptosis of enterocytes has been associated with increased epithelial permeability in doxorubicin-treated rats (53) and in camptothecin-treated colonic epithelial monolayers (6). More-

* Corresponding author. Mailing address: Department of Biological Sciences, University of Calgary, 2500 University Dr. N.W., Calgary, Alberta T2N 1N4, Canada. Phone: (403) 220-8573. Fax: (403) 289-9311. E-mail: aburet@ucalgary.ca.

over, immune-mediated apoptosis resulting from Fas cross-linking or from administration of tumor necrosis factor alpha increases permeability in human epithelial monolayers (1, 25). A number of enteric bacterial pathogens, including *Salmonella* sp., *Escherichia coli*, *Shigella*, and *Clostridium difficile* have the ability to induce enterocyte apoptosis (22, 33, 34, 37). Infection of colonic enterocytes with the protozoan parasite *Cryptosporidium parvum* can also induce apoptosis (41). However, the effects of *G. lamblia* on enterocyte apoptosis remain unknown, and a possible link between microbially induced apoptosis and abnormal intestinal permeability has yet to be established.

In an attempt to address these issues, the aims of the present study were as follows: (i) to assess whether *G. lamblia* can induce apoptosis in nontransformed human small intestinal epithelial cells, (ii) to investigate the effects of *G. lamblia* on tight junctional ZO-1 and permeability in human epithelial monolayers, and (iii) to determine whether *Giardia*-induced enterocyte apoptosis alters epithelial permeability.

MATERIALS AND METHODS

Cell culture model. All experiments were done with a novel nontransformed human duodenal epithelial cell line, SCBN. SCBN was the first nontumorigenic human small intestinal cell line to be grown as polarized confluent monolayers in vitro and has been shown to possess cytokeratins, mucin antigen, mRNA for epidermal growth factor, interleukin-6, vascular cell adhesion molecule-1, *Giardia*-sensitive cytoskeletal proteins, and calcium-dependent chloride secretion (9, 47, 55). Cells were grown in Dulbecco's modified Eagle medium (DMEM) (Sigma Chemical Co., St. Louis, Mo.), supplemented with 5% heat-inactivated fetal bovine serum, 100 μg of streptomycin/ml, 100 U of penicillin/ml, 0.08 mg of tylosin/ml, and 200 mM L-glutamine (all from Sigma) as described previously (55). Cells were incubated at 37°C and 5% CO_2 in 96% humidity. The culture medium was replenished every 2 to 3 days, and the cells were passaged with 2× trypsin-EDTA (Sigma). Trypsinized cells (2.0×10^5 cells/ml) were added to Lab-Tek chamber slides (Nalge Nunc International, Naperville, Ill.) (400 μl), to 12-well tissue culture-treated plates (Costar, Cambridge, Mass.) (500 μl), or to Snapwell filter units (Costar) (500 μl) which contained a 1.13-cm^2 semipermeable filter membrane with 0.4-μm pores. Each Snapwell filter unit was incubated in six-well cluster plates (Costar). In all studies, SCBN cells were used between passages 23 and 27.

Parasites. *G. lamblia* strain NF was obtained from an epidemic outbreak of human giardiasis in Newfoundland, Canada (55), strain WB was isolated from a symptomatic patient with chronic giardiasis who failed to respond to several courses of metronidazole treatment (52), and strain PB was isolated from a symptomatic patient from Portland, Oreg. (43). The *G. lamblia* strain S2 was originally isolated from a sheep (10). Recent studies have shown that SCBN monolayers exhibit similar cytoskeletal and electrical resistance abnormalities when challenged with either live *Giardia* trophozoites, *Giardia* sonicates, or spent *Giardia* growth media of either NF or S2 isolates (55). For the purpose of using a reproducible stimulus, and in order to avoid the physical interference of whole live parasites with permeability parameters, *Giardia* sonicates were used as the challenge in the present study. In addition, the scanning electron microscopy and the Hoechst fluorescence studies used live *Giardia* trophozoites. *Giardia* trophozoites were grown axenically at 37°C in Diamond's TY1-S-33 media (16) supplemented with 2.5 mg of piperacillin (Pipracil; Wyeth-Ayerst Canada Inc., Montreal, Quebec, Canada)/ml in 15-ml polystyrene centrifuge tubes (Falcon; Becton Dickinson and Co., Franklin Lakes, N.J) and subcultured every 7 days to maintain the lines. When harvesting the trophozoites, media and dead parasite sediments were removed by aspiration and the tube was filled with 4°C sterile phosphate-buffered saline (PBS). The live trophozoites were harvested at log phase (48 h) by cold shock on ice for 20 min followed by centrifugation at 500 × *g* for 10 min at 4°C. The pellet was washed once with 4°C PBS and then resuspended with 2 ml of 5% DMEM prior to challenge. The trophozoite concentration was determined with a hemocytometer and adjusted to 2×10^7 trophozoites/ml per well. To prepare the trophozoite sonicate, trophozoite suspensions (2×10^7 trophozoites/ml) were disrupted (550 Versonic Dismembrator; Fisher Scientific, Pittsburgh, Pa.) on ice with three bursts of 30 s each.

Experimental design. For the assessment of enterocyte apoptosis (Hoechst fluorescence staining, enzyme-linked immunosorbent assay [ELISA], electron microscopy) and characterization of tight junctional ZO-1, epithelial monolayers were used 5 days after passage, a time at which they had reached confluence but not overgrowth on their plastic substrates. For the measurement of epithelial permeability in Snapwell filter units, epithelial monolayers were used 7 days after passage, a time at which they are known to reach peak electrical resistance (>1,000 Ω/cm^2) (data not shown) on semipermeable membranes. Cells were incubated with *Giardia* trophozoites or sonicates for 24 h or for an additional 24 h with freshly prepared *Giardia* sonicates for assessments at 48 h. Enterocyte apoptosis was determined by incubating cell monolayers with either 5% DMEM (control) or 2.0×10^7 freshly sonicated trophozoites in 5% DMEM. In the experiments assessing apoptotic nucleosome quantification, tight junctional ZO-1, and epithelial permeability, monolayers were pretreated for 1 h at 37°C and 5% CO_2 with either 0.8% dimethyl sulfoxide (DMSO) vehicle or membrane-permeable 120 μM caspase-3 inhibitor II {Z-Asp(OCH_3)-Glu(OCH_3)-Val-Asp(OCH_3)-FMK [Z-DEVD-FMK]; Calbiochem, La Jolla, Calif.}, which is known to irreversibly inhibit apoptosis (45). Monolayers were washed once with tissue culture grade PBS (Sigma) to remove DMSO or caspase-3 inhibitor and then coincubated with either 5% DMEM (control) or 2.0×10^7 freshly sonicated trophozoites in 5% DMEM.

Scanning electron microscopy. For characterization of surface cellular abnormalities induced by *G. lamblia* (NF), preparations were examined by scanning electron microscopy. After 24 h of incubation (37°C, 5% CO_2, 96% humidity) with either 5% DMEM or sonicated or live *G. lamblia* (NF), monolayers were fixed in 2% glutaraldehyde (Electron Microscopy Sciences, Fort Washington, Pa.), postfixed in 2% osmium tetroxide (JBS Supplies, JB EM Services Inc., Dorval, Quebec, Canada), dehydrated in ethanol and freon, sputter coated with gold-palladium, and mounted on aluminum stubs. Photomicrographs were obtained with a Hitachi 450 scanning electron microscope (Hitachi Scientific Instruments, Mississauga, Ontario, Canada) at an acceleration voltage of 20 kV.

Transmission electron microscopy. The effects of *G. lamblia* on enterocyte apoptosis were further assessed by transmission electron microscopy. After 24 h of incubation (37°C, 5% CO_2, 96% humidity) with either 5% DMEM or *G. lamblia* (NF) sonicates in 5% DMEM, confluent monolayers were fixed in 5% glutaraldehyde (Electron Microscopy Sciences), postfixed in 1% osmium tetroxide (JBS Supplies), dehydrated in ethanol, cleared in propylene oxide, and embedded in Spurr low-viscosity medium (Electron Microscopy Sciences). Thin sections (90 nm) were stained with saturated uranyl acetate in 50% aqueous ethanol and 0.04% (wt/vol) lead citrate. Photomicrographs were obtained with a Hitachi H-7000 transmission electron microscope at an acceleration voltage of 80 kV. Enterocytes with signs of apoptosis (i.e., condensed nuclear chromatin, nuclear membrane delamination, cytoplasmic vacuolation, and/or accumulation of zymogen granules) were identified.

Hoechst fluorescent staining. Nuclear staining was performed as another marker of apoptosis in SCBN monolayers grown on chamber slides (Nalge Nunc) for 5 days as described above. After 24 h of challenge, cells were stained with the membrane-permeable and nuclear-specific fluorescent dye Hoechst (1 μM; Molecular Probes, Eugene, Oreg.) (10 min, room temperature). After three PBS washes (5 min, room temperature), the chamber wells were filled with PBS. Cells were visualized on a Leica DMR inverted fluorescence microscope. The numbers of stained enterocytes that exhibited apoptotic nuclear condensation and fragmentation were counted in three distinct areas of each slide, and percentages were calculated. The concentration of apoptotic enterocytes in *Giardia*-stimulated wells was expressed as a ratio to that of the controls. Photomicrographs were taken on a Photometrics CoolSNAP digital camera (Roper Scientific, Tucson, Ariz.).

Apoptotic nucleosome quantification. Enterocyte apoptosis was quantified as outlined in the experimental design by using a cell death detection ELISA kit (Roche Molecular Biochemicals, Laval, Quebec, Canada) according to the manufacturer's instructions. This quantitative sandwich enzyme immunoassay specifically measures the histone region (H1, H2A, H2B, H3, and H4) of mono- and oligonucleosomes that are released during apoptosis. Enterocyte apoptosis in the monolayers was calculated 8, 24, and 48 h after challenge. The proapoptotic topoisomerase-I inhibitor camptothecin (20 μg/ml; Sigma) was used as a positive control for apoptosis after 24 h of incubation. Photometric development was monitored kinetically by reading the plate at 405 nm at 5-min intervals by using a THERMOmax microplate reader (Molecular Devices Corp., Menlo Park, Calif.). Apoptosis was measured in duplicate from 10^5 enterocytes from each group and expressed as a ratio of the absorbance of the experimental cell lysates to that of controls (which was arbitrarily set at 1.0) after 30 min of development. The detection limit for this ELISA is 10^2 apoptotic cells.

Tight junctional ZO-1 immunofluorescence. Monolayers grown in chamber slides (Nalge Nunc) for 5 days were used to determine the effects of *G. lamblia* (NF) on tight junctional ZO-1 integrity 24 h postinoculation. To assess whether

changes were due to apoptosis, experiments characterized the effects of the caspase-3 inhibitor, Z-DEVD-FMK, on the *G. lamblia*-induced alterations to tight junctional ZO-1. Monolayers were fixed with fresh 2% paraformaldehyde (Polysciences, Warrington, Pa.) in PBS (2 h, room temperature) and washed three times with PBS (10 min, room temperature). Cells were permeabilized with 0.5% Triton X-100 (Sigma) (15 min, room temperature) and washed three times with PBS (10 min, room temperature). Nonspecific antibody binding was blocked with fetal bovine serum (undiluted concentration; Sigma) (10 min, room temperature) and washed three times with PBS (10 min, room temperature). Then the monolayers were incubated (37°C, 1 h, humid chamber) with affinity-purified polyclonal rabbit anti-ZO-1 (1:100 in PBS; Zymed Laboratories, San Francisco, Calif.) and washed three times with PBS (10 min, room temperature). Next, the monolayers were incubated (37°C, 1 h, dark humid chamber) with Cy3-conjugated sheep anti-rabbit immunoglobulin G (1:100 in PBS; Sigma) and washed three times with PBS (10 min, room temperature). Finally, monolayers were mounted with Aqua Poly-Mount (Polysciences) and viewed under a View Scan DVC-250 confocal laser scanning microscope (Bio-Rad Laboratories, Hercules, Calif.). Photomicrographs were obtained with a Spot II digital camera (Diagnostic Instruments Inc., Sterling Heights, Mich.).

Epithelial permeability. To confirm monolayer confluence, transepithelial resistance was measured with an electrovoltohmeter (World Precision Instruments, Sarasota, Fla.) in six separate monolayers grown on Snapwell filter units (Costar) prior to the study. Each monolayer reached a peak resistance of $>1{,}000\ \Omega/cm^2$ by day 7. Electrical resistance was not measured in subsequent studies to avoid any possible disruption of the epithelial barrier integrity prior to experimentation. Effects of *Giardia* on barrier function were evaluated in the absence or presence of the caspase-3 inhibitor Z-DEVD-FMK in monolayers prepared as described above. Epithelial permeability to a dextran probe (3,000 MW) was assessed by using methods described previously (24). Briefly, at 24 and 48 h postinoculation, the apical and basolateral compartments were washed gently two times with sterile bicarbonate-buffered Ringer's solution (37°C). A nonabsorbable fluorescein isothiocyanate (FITC)-conjugated dextran probe (100 μM in Ringer's solution, 3,000 MW; Molecular Probes) was added to the apical compartment, and Ringer's solution was added to the basolateral compartment. After 3 h of incubation (37°C, 5% CO_2, 96% humidity), two 300-μl samples were collected from the basolateral compartment. Relative fluorescence units of the samples were calculated with a microplate fluorometer (Spectra Max Gemini). Values were expressed as percent apical FITC-dextran $\times\ 10^{-3}$ per centimeter^2 per hour that crossed the Snapwell membrane (24).

Statistical analysis. Results were expressed as means ± standard errors of the means and compared by one-way analysis of variance followed by Tukey's test for multiple comparison analysis where applicable. Statistical significance was established at a P value of <0.05.

RESULTS

Enterocyte apoptosis. The first series of experiments assessed the effects of *G. lamblia* sonicates on enterocyte apoptosis. Initially, monolayers were incubated with live *G. lamblia* (NF) trophozoites for 24 h and prepared for scanning electron microscopy. Compared to controls, monolayers exposed to *G. lamblia* trophozoites or sonicates exhibited focal blebbing of the apical membrane, a characteristic feature of enterocyte apoptosis (Fig. 1).

Under transmission electron microscopy, control monolayers exhibited intact nuclear and cellular ultrastructure (Fig. 2A). In contrast, monolayers coincubated with *G. lamblia* (NF) sonicates contained a number of enterocytes with ultrastructural evidence of cell death. Apoptotic cells were characterized by intact cellular membranes and organelles, cytosolic accumulation of zymogen granules, cytoplasmic vacuolation, chromatin condensation, and nuclear membrane delamination (Fig. 2B and C).

In order to quantify the apoptotic changes induced by *G. lamblia*, monolayers were incubated with the membrane-permeable Hoechst fluorescent dye and assessed for apoptotic nuclear changes. After 24 h of incubation, control monolayers exhibited characteristically uniform fluorescent nuclear staining throughout all nuclei (Fig. 3A). In contrast, exposure to *G. lamblia* NF or S2 increased the incidence of nuclear condensation and fragmentation by approximately three- and fourfold, respectively (Fig. 3F), as shown by intense fluorescent staining within areas of the nucleus in comparison to controls (Fig. 3B and C). In contrast, monolayers incubated with *G. lamblia* WB or PB had nuclear staining profiles similar to those of the controls (Fig. 3D to F). To address whether live trophozoites induce similar apoptotic changes, separate experiments showed that live trophozoites induced significant nuclear condensation (NF, 5.90% ± 0.47, $n = 6$; S2, 6.25% ± 0.79, $n = 6$)

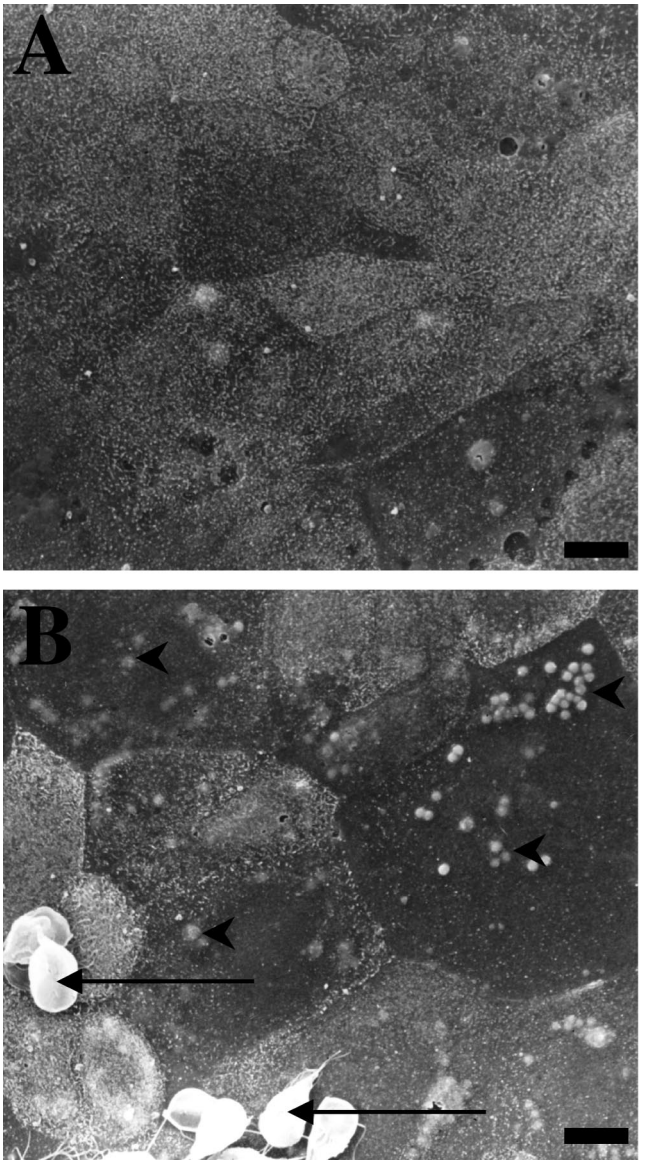

FIG. 1. Representative scanning electron micrographs of nontransformed human duodenal epithelial SCBN monolayers coincubated with either 5% DMEM growth media (A) or *G. lamblia* (NF) trophozoites in 5% DMEM (B) for 24 h. Monolayers incubated with *G. lamblia* trophozoites (arrows) exhibit high incidences of focal surface membrane blebbing (arrowheads) and less distinct microvilli. Similar alterations were observed when monolayers were incubated with NF trophozoite sonicates for 24 h (data not shown). Bars = 5 μm.

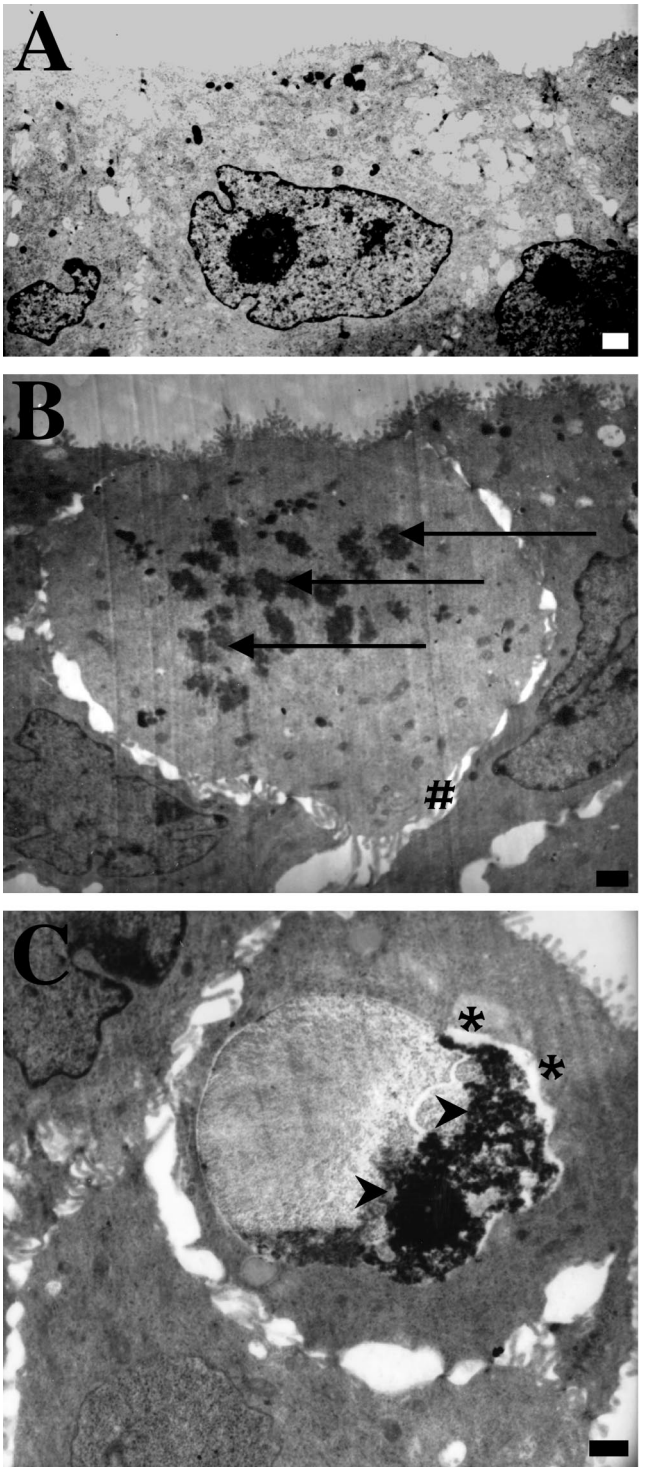

FIG. 2. Representative transmission electron micrographs illustrating nontransformed human duodenal epithelial SCBN monolayers incubated (for 24 h) with either 5% DMEM growth media (A) or *G. lamblia* sonicates (NF) (B and C). (A) Sham-treated enterocytes exhibit intact nuclear structures. (B and C) Cells coincubated with *G. lamblia* sonicates exhibit ultrastructural features of apoptotic cells characterized by intact organelles and cellular membranes (#), accumulation of zymogen granules (arrows), cytoplasmic vacuolation, chromatin condensation (arrowheads), and nuclear membrane delamination (*). Bars = 1 μm.

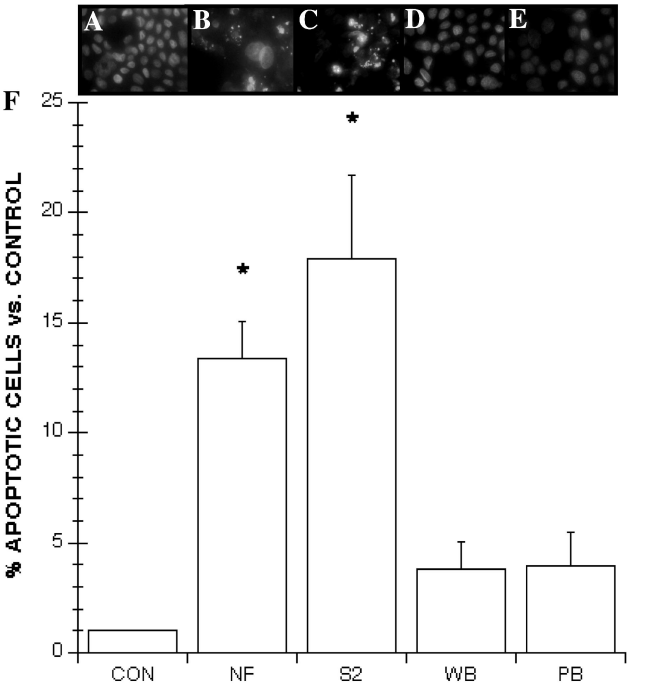

FIG. 3. Representative fluorescence photomicrographs and results obtained from the Hoechst fluorescence assay for enterocyte apoptosis. Photographs were taken at the same magnification (× 400). Nontransformed human duodenal epithelial SCBN monolayers were incubated for 24 h with either 5% DMEM growth media (A), *G. lamblia* NF sonicates (B), *G. lamblia* S2 sonicates (C), *G. lamblia* WB sonicates (D), or *G. lamblia* PB sonicates (E). Control cells exhibit diffuse staining of Hoechst throughout the nucleus (A). Cells coincubated with *G. lamblia* NF or S2 exhibit nuclear condensation and fragmentation (B and C). In contrast, *G. lamblia* WB and PB strains did not induce nuclear condensation or fragmentation (D and E). (F) Apoptotic ratios of SCBN enterocytes incubated for 24 h with NF ($n = 14$), S2 ($n = 13$), WB ($n = 8$), or PB ($n = 8$) *G. lamblia* sonicates. Values were calculated as percent ratios versus values measured in control monolayers (CON) incubated with 5% DMEM growth media ($n = 13$) (arbitrarily set at 1.0). Values are means ± standard errors of the means. *, $P < 0.05$ versus control.

in comparison to controls (expressed as 1.00%, $n = 6$) after 24 h of incubation.

Additional experiments further quantified apoptotic changes by measuring the production of apoptotic nucleosomes from enterocytes exposed to *Giardia*. After 24 or 48 h of incubation, *G. lamblia* NF and S2 significantly increased the induction of apoptosis within monolayers (Fig. 4). In contrast, the degree of enterocyte apoptosis in monolayers exposed for 24 or 48 h to *G. lamblia* WB or PB did not significantly differ from that of the controls (Fig. 4). Levels of apoptosis induced by *G. lamblia* NF and S2 were similar to those obtained after 24 h of incubation with the proapoptotic compound camptothecin (Fig. 4). In order to provide direct evidence that the caspase-3 inhibitor Z-DEVD-FMK prevents apoptosis, monolayers were pretreated with Z-DEVD-FMK prior to probing for apoptosis. Pretreatment with Z-DEVD-FMK significantly prevented the induction of apoptosis by *G. lamblia* NF (24 and 48 h) and S2 (24 h) (Fig. 4) and maintained control baseline levels of apoptosis in monolayers incubated with WB (24 h, 0.42 ± 0.12, $n = 12$; 48 h, 0.82 ± 0.10, $n = 12$) or PB isolates (24 h, 0.53 ±

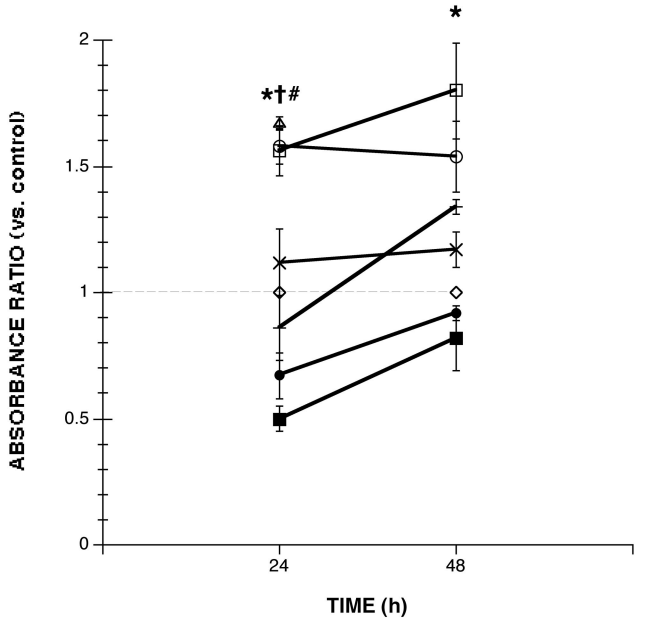

FIG. 4. Levels of enterocyte apoptosis in human duodenal epithelial monolayers incubated with either 5% DMEM growth media alone (◇) ($n = 15$ at 24 h, $n = 9$ at 48 h), *G. lamblia* NF in 5% DMEM (□) ($n = 9$ to 15), strain S2 sonicates (○) ($n = 9$ to 15), strain WB sonicates (×) ($n = 3$), strain PB sonicates (+) ($n = 3$), or 20 μg of camptothecin/ml (△) ($n = 6$). Apoptotic ratios were also calculated for monolayers pretreated with Z-DEVD-FMK followed by incubation with *G. lamblia* NF (■) ($n = 6$ at 24 h, $n = 6$ at 48 h) or S2 sonicates (●) ($n = 6$ at 24 h, $n = 6$ at 48 h). Values after 30 min of ELISA development were calculated as absorbance ratios versus values measured in control monolayers (arbitrarily set at 1.0) (◇). NF and S2 isolates increased the production of apoptotic nucleosomes to levels induced by proapoptotic camptothecin and to levels greater than those in negative controls, whereas WB and PB isolates did not. Pretreatment with Z-DEVD-FMK prevented the induction of apoptosis by NF and S2 isolates. Values are means ± standard errors of the means. *, $P < 0.05$ for NF versus control; =, $P < 0.05$ for S2 versus control; #, $P < 0.05$ versus control.

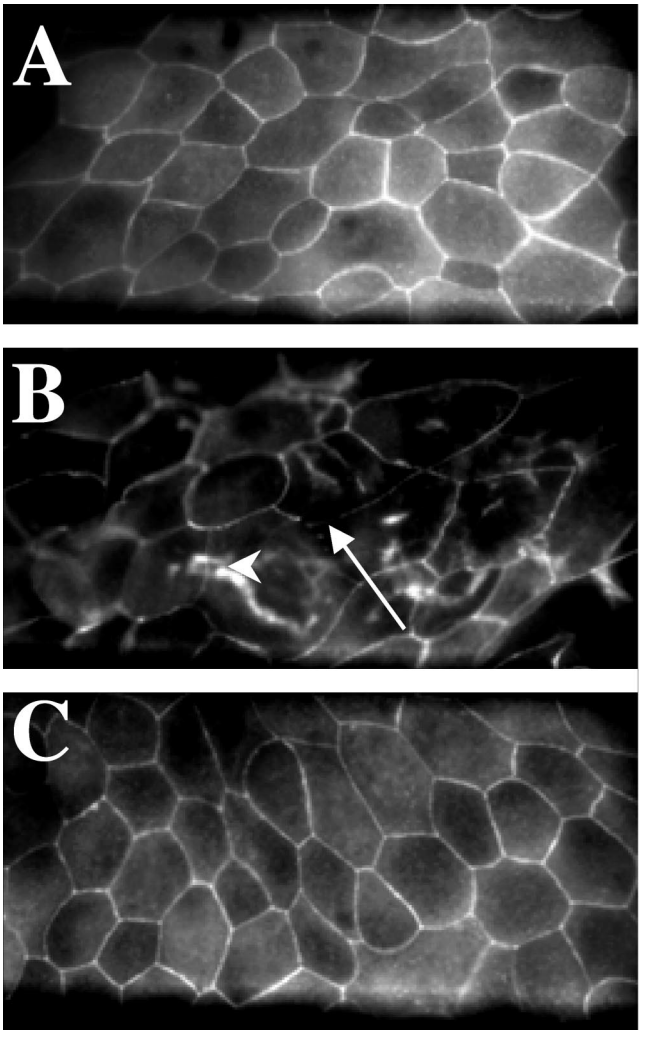

FIG. 5. Representative confocal scanning laser micrographs illustrating ZO-1 integrity in human duodenal epithelial monolayers. Preparations were coincubated with either 5% DMEM growth media following pretreatment with DMSO vehicle (A), *G. lamblia* NF sonicates for 24 h following pretreatment with DMSO vehicle (B), or *G. lamblia* NF strain sonicates for 24 h following pretreatment with the caspase-3 inhibitor Z-DEVD-FMK (C). Control monolayers exhibit typical continuous ZO-1 pericellular organization at the periphery of individual enterocytes. Monolayers incubated with NF strain sonicates exhibit focal disruption of ZO-1 along the pericellular junctions (arrow), and punctate ZO-1 redistribution (arrowhead) throughout the monolayer. Pretreatment with a caspase-3 inhibitor prevents the ZO-1 disruption induced by *G. lamblia*. Magnification, ×600.

0.11, $n = 12$; 48 h, 0.80 ± 0.18, $n = 12$). Since the induction of apoptosis by NF and S2 isolates appeared to be similar at 24 and 48 h, apoptosis was assessed earlier, at 8 h, to determine whether there is a time-dependent induction of apoptosis. Detectable levels of apoptosis were not observed by ELISA after 8 h of incubation with either *G. lamblia* NF (0.77 ± 0.04; $n = 12$) or S2 (0.72 ± 0.03; $n = 12$) sonicates.

Tight junctional ZO-1. Additional experiments assessed the effects of *G. lamblia* on tight junctional ZO-1 integrity and determined whether these effects could be blocked by the caspase-3 inhibitor Z-DEVD-FMK in an attempt to establish a link between epithelial injury and apoptosis. *G. lamblia* NF was selected for the experimental challenge since it reproducibly induced enterocyte apoptosis in the previous experiments. Analysis of monolayers exposed to *G. lamblia* revealed focal disruptions and punctate concentrations of ZO-1 along the pericellular junctions, and migration of ZO-1 towards the nuclei 24 h postchallenge (Fig. 5). Pretreatment with Z-DEVD-FMK prior to incubation with *Giardia* sonicates prevented these abnormalities and maintained the continuous pericellular organization of ZO-1 typical of control monolayers (Fig. 5). Monolayers pretreated with Z-DEVD-FMK alone were not different from the controls (data not shown).

Epithelial permeability. The effects of *G. lamblia* NF on transepithelial permeability, with or without caspase-3 inhibitor pretreatment, were assessed on SCBN monolayers grown on Snapwell filter units. After 7 days of culture and 24 h of incubation with vehicle alone, control monolayers developed a tight epithelial barrier as shown by low transepithelial FITC-dextran fluxes into the basolateral compartment [(54.0 ± 10.0)% apical FITC-dextran × 10^{-3} cm^{-2} h^{-1}] (Fig. 6A). In contrast, in monolayers coincubated with trophozoite sonicates for 24 h, transepithelial fluxes of FITC-dextran were increased

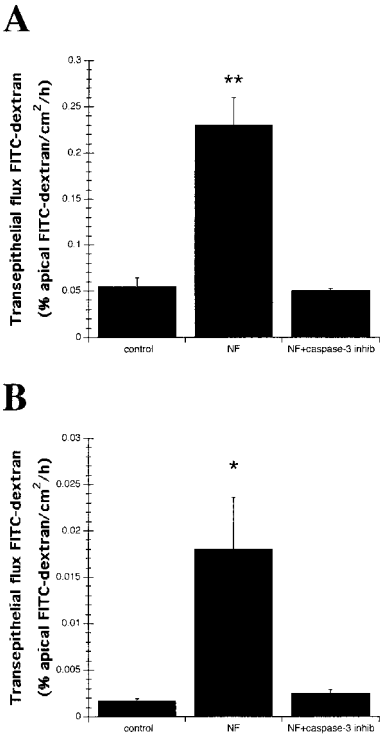

FIG. 6. Transepithelial fluxes of FITC-dextran 3000 across nontransformed human duodenal epithelial SCBN monolayers incubated with either 5% DMEM, *G. lamblia* NF sonicates, or *G. lamblia* sonicates after pretreatment with the caspase-3 inhibitor Z-DEVD-FMK 24 (A) and 48 (B) h postinoculation. Exposure to *G. lamblia* significantly increases transepithelial permeability. Pretreatment with a caspase-3 inhibitor abolishes the *Giardia*-induced effect. Values are means ± standard errors of the means ($n = 4$ per group). *, $P < 0.05$; **, $P < 0.01$ versus control.

more than fourfold [(230.0 ± 30.0)% apical FITC-dextran × 10^{-3} cm^{-2} h^{-1}] (Fig. 6A) in comparison to control values. Pretreatment with the caspase-3 inhibitor Z-DEVD-FMK prevented the *G. lamblia*-induced increase in transepithelial flux of FITC-dextran [(50.0 ± 3.0)% apical FITC-dextran × 10^{-3} cm^{-2} h^{-1}] (Fig. 6A) across the monolayer and maintained fluxes similar to those of the controls. Further studies measured epithelial permeability at 48 h (Fig. 6B). While all monolayers treated for 48 h exhibited lower transepithelial FITC-dextran fluxes than those measured at 24 h, transepithelial fluxes in monolayers exposed to *Giardia* sonicates were again significantly higher than those measured in the controls. Similar to the trend observed at 24 h postinoculation, pretreatment with Z-DEVD-FMK prevented this increase in FITC-dextran flux and maintained values similar to those of the controls. Incubation with Z-DEVD-FMK alone had no effect on permeability at either time of experimentation.

DISCUSSION

Results from this study demonstrate that *G. lamblia* induces apoptosis in small intestinal epithelial cells in a strain-dependent manner. In addition, *G. lamblia* disrupts tight junctional ZO-1 and increases epithelial permeability across epithelial monolayers. In addition to inhibiting apoptosis, pretreatment of epithelial cells with the caspase-3 inhibitor Z-DEVD-FMK prevented both the disruption of tight junctional ZO-1 and the increase in epithelial permeability. Together, the findings indicate that strain-dependent *Giardia*-induced enterocyte apoptosis is responsible for the loss of epithelial barrier function and that these alterations are caspase-3 dependent.

A variety of microbial pathogens, such as *Salmonella* sp., *E. coli*, *Shigella* sp., *C. difficile*, *Listeria monocytogenes*, and *C. parvum*, have been shown to induce enterocyte apoptosis (22, 33, 34, 41, 56). Findings from this study demonstrate for the first time that the protozoan parasite *G. lamblia* has the capability to cause apoptosis in small intestinal epithelial cells. Moreover, the four isolates used in this study differed in their ability to induce enterocyte apoptosis. This observation is consistent with a recent report which indicated that small intestinal injury in neonatal rats infected with *G. lamblia* was strain dependent (14). The relatively moderate levels of apoptosis induced by *G. lamblia* are similar to those reported for human colonic enterocytes exposed to *C. parvum* (41). It is well established that cell death by apoptosis contributes to the resolution of inflammation (28). The proapoptotic effects of *G. lamblia* may perhaps explain the lack of inflammatory infiltration in intestinal tissues colonized by this parasite, and this observation requires further investigation.

Epithelial barrier function prevents luminal contents from having detrimental effects on subepithelial tissues and, hence, plays an essential role in the maintenance of intestinal homeostasis. A number of gastrointestinal disorders, including inflammatory bowel disease, celiac disease, and bacterial enteritis, are associated with a breakdown of epithelial barrier integrity (5, 21, 31, 32). Studies have shown that *C. difficile* toxin A, as well as gamma interferon, may disorganize F-actin and disrupt ZO-1 integrity, which in turn increases transepithelial permeability (29, 58). Other experiments demonstrated that *G. lamblia* induces a rearrangement of cytoskeletal F-actin and α-actinin in human colonic Caco-2 and duodenal epithelial SCBN monolayers, and these changes were associated with a decrease in transepithelial electrical resistance (55). Consistent with these observations, the present findings reveal that *G. lamblia* may disrupt tight junctional ZO-1 and increase transepithelial permeability for the luminal probe dextran 3000. Intriguingly, increased intestinal permeability may also be induced by proapoptotic drugs such as doxorubicin and camptothecin (6, 53). In addition, recent studies have established that immune-mediated apoptosis induced by Fas or tumor necrosis factor alpha is responsible for increased transepithelial permeability (1, 25). The results reported herein demonstrate for the first time that microbially induced enterocyte apoptosis may cause a loss of intestinal barrier function, as both the disruption of tight junctional ZO-1 and the increased epithelial permeability for dextran induced by *Giardia* were abolished by the inhibition of caspase-3.

In the epithelium, cytoskeletal integrity plays a central role in ensuring cell survival by maintaining tight contacts with the extracellular matrix and other neighboring cells (3, 42). The cleavage of cytoskeletal proteins, such as actin, α-fodrin, and keratin, by caspases is responsible for the structural disintegration and membrane blebbing observed in apoptotic cells (13, 36, 39, 40). In addition, cleavage of proteins which regulate cytoskeletal assembly, such as gelsolin and growth arrest-spe-

cific gene product 2 (Gas2), as well as breakdown of cytoproliferative proteins such as Ras GTPase activating protein (RasGAP), may also actively promote the morphological changes observed in apoptotic cells. These alterations include disruption of the actin cytoskeleton and cellular rounding, ultimately leading to detachment from the substrate (7, 35, 57). Caspase-dependent cleavage of adherens junctional components, such as β-catenin and plakoglobin, facilitates the detachment of apoptotic cells (8, 30, 50). Findings from this study indicate that *Giardia*-induced disruption of tight junctional ZO-1 is caspase-3 dependent. These results are consistent with previous observations which showed that induction of apoptosis in colonic T84 monolayers by Fas cross-linking was associated with disturbances in tight junctional protein ZO-1 and desmoplakins 1 and 2 (1). In these studies, pretreatment with a pan caspase inhibitor (Z-VAD-FMK) prevented changes to ZO-1 induced by proapoptotic Fas cross-linking (1). Future experiments studying the enzyme-substrate relationship between caspase-3 and tight junctional proteins such as ZO-1 could further support the role of caspases in regulating paracellular permeability.

This study used *Giardia* extracts obtained from sonicated trophozoites as the stimuli for epithelial injury. While it is well established that *Giardia* is a noninvasive intestinal pathogen, studies have shown that *Giardia* trophozoites possess proteases that may be involved in pathogenesis (27, 46, 48). Moreover, excretory-secretory products produced by *G. lamblia* may reduce D-glucose and L-phenylalanine uptake in brush border vesicles and induce the net secretion of sodium and chloride when administered directly to intestinal tissues in mice (49). Other studies have shown that fractions of *G. lamblia* trophozoites may induce disaccharidase deficiencies in gerbils (4, 44). Moreover, genes found in some *G. lamblia* isolates contain multiple repeats of a snake toxin homologue (15). Although possible virulence factors possessed by *Giardia* have yet to be uncovered, findings from this study further support the hypothesis that the pathophysiology of giardiasis implicates parasitic factors which may induce apoptosis, disrupt tight junctional ZO-1, and increase epithelial permeability in a strain-dependent manner.

In summary, results from the present study report strain-dependent induction of enterocyte apoptosis by *G. lamblia* trophozoite extracts. Perhaps more importantly, the findings also demonstrate for the first time that microbially induced apoptosis in enterocytes correlates with the loss of epithelial barrier function in small intestinal monolayers, via the disruption of tight junctional ZO-1 and the subsequent increase in permeability, and that this injury is caspase-3 dependent. Future studies will determine whether strains of *Giardia* that cause apoptosis also induce greater intestinal damage and more-severe symptoms in vivo.

ACKNOWLEDGMENTS

This work was funded by the Natural Sciences and Engineering Research Council of Canada and the Crohn's and Colitis Foundation of Canada. Research by J.B.M. and W.K.M. is sponsored by the Alberta Heritage Foundation for Medical Research and the Canadian Institutes of Health Research.

We are grateful to Doug Muench for expert assistance in confocal laser microscopy.

REFERENCES

1. **Abreu, M. T., A. A. Palladino, E. T. Arnold, R. S. Kwon, and J. A. McRoberts.** 2000. Modulation of barrier function during Fas-mediated apoptosis in human intestinal epithelial cells. Gastroenterology **119:**1524–1536.
2. **Anderson, J. M., and C. M. Van Itallie.** 1995. Tight junctions and the molecular basis for regulation of paracellular permeability. Am. J. Physiol. **269:**G467–G475.
3. **Bates, R. C., A. Buret, D. F. van Helden, M. A. Horton, and G. F. Burns.** 1994. Apoptosis induced by inhibition of intercellular contact. J. Cell Biol. **125:**403–415.
4. **Belosevic, M., G. M. Faubert, and J. D. MacLean.** 1989. Disaccharidase activity in the small intestine of gerbils (Meriones unguiculatus) during primary and challenge infections with Giardia lamblia. Gut **30:**1213–1219.
5. **Bjarnason, I., A. MacPherson, and D. Hollander.** 1995. Intestinal permeability: an overview. Gastroenterology **108:**1566–1581.
6. **Bojarski, C., K. Bendfeldt, A. H. Gitter, J. Mankertz, M. Fromm, S. Wagner, E. O. Riecken, and J. D. Schulzke.** 2000. Apoptosis and intestinal barrier function. Ann. N. Y. Acad. Sci. **915:**270–274.
7. **Brancolini, C., M. Benedetti, and C. Schneider.** 1995. Microfilament reorganization during apoptosis: the role of Gas2, a possible substrate for ICE-like proteases. EMBO J. **14:**5179–5190.
8. **Brancolini, C., A. Sgorbissa, and C. Schneider.** 1998. Proteolytic processing of the adherens junctions components beta-catenin and gamma-catenin/plakoglobin during apoptosis. Cell Death Differ. **5:**1042–1050.
9. **Buresi, M. C., E. Schleihauf, N. Vergnolle, A. Buret, J. L. Wallace, M. D. Hollenberg, and W. K. MacNaughton.** 2001. Protease-activated receptor-1 stimulates Ca(2+)-dependent Cl(-) secretion in human intestinal epithelial cells. Am. J. Physiol. Gastrointest. Liver Physiol. **281:**G323–G332.
10. **Buret, A., N. denHollander, P. M. Wallis, D. Befus, and M. E. Olson.** 1990. Zoonotic potential of giardiasis in domestic ruminants. J. Infect. Dis **162:** 231–237.
11. **Buret, A., D. G. Gall, and M. E. Olson.** 1991. Growth, activities of enzymes in the small intestine, and ultrastructure of microvillous border in gerbils infected with Giardia duodenalis. Parasitol. Res. **77:**109–114.
12. **Buret, A., J. A. Hardin, M. E. Olson, and D. G. Gall.** 1992. Pathophysiology of small intestinal malabsorption in gerbils infected with Giardia lamblia. Gastroenterology **103:**506–513.
13. **Caulin, C., G. S. Salvesen, and R. G. Oshima.** 1997. Caspase cleavage of keratin 18 and reorganization of intermediate filaments during epithelial cell apoptosis. J. Cell Biol. **138:**1379–1394.
14. **Cevallos, A., S. Carnaby, M. James, and J. G. Farthing.** 1995. Small intestinal injury in a neonatal rat model of giardiasis is strain dependent. Gastroenterology **109:**766–773.
15. **Chen, N., J. A. Upcroft, and P. Upcroft.** 1995. A Giardia duodenalis gene encoding a protein with multiple repeats of a toxin homologue. Parasitology **111:**423–431.
16. **Diamond, L. S., D. R. Harlow, and C. C. Cunnick.** 1978. A new medium for the axenic cultivation of Entamoeba histolytica and other Entamoeba. Trans. R. Soc. Trop. Med. Hyg. **72:**431–432.
17. **Fanning, A. S., B. J. Jameson, L. A. Jesaitis, and J. M. Anderson.** 1998. The tight junction protein ZO-1 establishes a link between the transmembrane protein occludin and the actin cytoskeleton. J. Biol. Chem. **273:**29745–29753.
18. **Farthing, M. J.** 1996. Giardiasis. Gastroenterol. Clin. N. Am. **25:**493–515.
19. **Fasano, A.** 2001. Intestinal zonulin: open sesame! Gut **49:**159–162.
20. **Fasano, A., B. Baudry, D. W. Pumplin, S. S. Wasserman, B. D. Tall, J. M. Ketley, and J. B. Kaper.** 1991. Vibrio cholerae produces a second enterotoxin, which affects intestinal tight junctions. Proc. Natl. Acad. Sci. USA **88:**5242–5246.
21. **Fiocchi, C.** 1998. Inflammatory bowel disease: etiology and pathogenesis. Gastroenterology **115:**182–205.
22. **Fiorentini, C., A. Fabbri, L. Falzano, A. Fattorossi, P. Matarrese, R. Rivabene, and G. Donelli.** 1998. *Clostridium difficile* toxin B induces apoptosis in intestinal cultured cells. Infect. Immun. **66:**2660–2665.
23. **Furuse, M., T. Hirase, M. Itoh, A. Nagafuchi, S. Yonemura, and S. Tsukita.** 1993. Occludin: a novel integral membrane protein localizing at tight junctions. J. Cell Biol. **123:**1777–1788.
24. **Gerhard, R., G. Schmidt, F. Hofmann, and K. Aktories.** 1998. Activation of Rho GTPases by *Escherichia coli* cytotoxic necrotizing factor 1 increases intestinal permeability in Caco-2 cells. Infect. Immun. **66:**5125–5131.
25. **Gitter, A. H., K. Bendfeldt, J. D. Schulzke, and M. Fromm.** 2000. Leaks in the epithelial barrier caused by spontaneous and TNF-alpha-induced single-cell apoptosis. FASEB J. **14:**1749–1753.
26. **Hardin, J. A., A. G. Buret, M. E. Olson, M. H. Kimm, and D. G. Gall.** 1997. Mast cell hyperplasia and increased macromolecular uptake in an animal model of giardiasis. J. Parasitol. **83:**908–912.
27. **Hare, D. F., E. L. Jarroll, and D. G. Lindmark.** 1989. Giardia lamblia: characterization of proteinase activity in trophozoites. Exp. Parasitol. **68:** 168–175.
28. **Haslett, C.** 1997. Granulocyte apoptosis and inflammatory disease. Br. Med. Bull. **53:**669–683.
29. **Hecht, G., C. Pothoulakis, J. T. LaMont, and J. L. Madara.** 1988. Clostrid-

ium difficile toxin A perturbs cytoskeletal structure and tight junction permeability of cultured human intestinal epithelial monolayers. J. Clin. Investig. **82:**1516–1524.
30. **Herren, B., B. Levkau, E. W. Raines, and R. Ross.** 1998. Cleavage of beta-catenin and plakoglobin and shedding of VE-cadherin during endothelial apoptosis: evidence for a role for caspases and metalloproteinases. Mol. Biol. Cell **9:**1589–1601.
31. **Hollander, D.** 1988. Crohn's disease–-a permeability disorder of the tight junction? Gut **29:**1621–1624.
32. **Isolauri, E., M. Juntunen, S. Wiren, P. Vuorinen, and T. Koivula.** 1989. Intestinal permeability changes in acute gastroenteritis: effects of clinical factors and nutritional management. J. Pediatr. Gastroenterol. Nutr. **8:**466–473.
33. **Keenan, K. P., D. D. Sharpnack, H. Collins, S. B. Formal, and A. D. O'Brien.** 1986. Morphologic evaluation of the effects of Shiga toxin and E. coli Shiga-like toxin on the rabbit intestine. Am. J. Pathol. **125:**69–80.
34. **Kim, J. M., L. Eckmann, T. C. Savidge, D. C. Lowe, T. Witthoft, and M. F. Kagnoff.** 1998. Apoptosis of human intestinal epithelial cells after bacterial invasion. J. Clin. Investig. **102:**1815–1823.
35. **Kothakota, S., T. Azuma, C. Reinhard, A. Klippel, J. Tang, K. Chu, T. J. McGarry, M. W. Kirschner, K. Koths, D. J. Kwiatkowski, and L. T. Williams.** 1997. Caspase-3-generated fragment of gelsolin: effector of morphological change in apoptosis. Science **278:**294–298.
36. **Ku, N. O., J. Liao, and M. B. Omary.** 1997. Apoptosis generates stable fragments of human type I keratins. J. Biol. Chem. **272:**33197–33203.
37. **Mahida, Y. R., S. Makh, S. Hyde, T. Gray, and S. P. Borriello.** 1996. Effect of Clostridium difficile toxin A on human intestinal epithelial cells: induction of interleukin 8 production and apoptosis after cell detachment. Gut **38:**337–347.
38. **Marshall, M. M., D. Naumovitz, Y. Ortega, and C. R. Sterling.** 1997. Waterborne protozoan pathogens. Clin. Microbiol. Rev. **10:**67–85.
39. **Martin, S. J., G. A. O'Brien, W. K. Nishioka, A. J. McGahon, A. Mahboubi, T. C. Saido, and D. R. Green.** 1995. Proteolysis of fodrin (non-erythroid spectrin) during apoptosis. J. Biol. Chem. **270:**6425–6428.
40. **Mashima, T., M. Naito, N. Fujita, K. Noguchi, and T. Tsuruo.** 1995. Identification of actin as a substrate of ICE and an ICE-like protease and involvement of an ICE-like protease but not ICE in VP-16-induced U937 apoptosis. Biochem. Biophys. Res. Commun. **217:**1185–1192.
41. **McCole, D. F., L. Eckmann, F. Laurent, and M. F. Kagnoff.** 2000. Intestinal epithelial cell apoptosis following *Cryptosporidium parvum* infection. Infect. Immun. **68:**1710–1713.
42. **Meredith, J. E., Jr., B. Fazeli, and M. A. Schwartz.** 1993. The extracellular matrix as a cell survival factor. Mol. Biol. Cell **4:**953–961.
43. **Meyer, E. A.** 1976. Giardia lamblia: isolation and axenic cultivation. Exp. Parasitol. **39:**101–105.
44. **Mohammed, S. R., and G. M. Faubert.** 1995. Purification of a fraction of Giardia lamblia trophozoite extract associated with disaccharidase deficiencies in immune Mongolian gerbils (Meriones unguiculatus). Parasite **2:**31–39.
45. **Nicholson, D. W., A. Ali, N. A. Thornberry, J. P. Vaillancourt, C. K. Ding, M. Gallant, Y. Gareau, P. R. Griffin, M. Labelle, Y. A. Lazebnik, et al.** 1995. Identification and inhibition of the ICE/CED-3 protease necessary for mammalian apoptosis. Nature **376:**37–43.
46. **North, M. J., J. C. Motram, and G. H. Coombs.** 1990. Cysteine proteinases of parasitic protozoa. Parasitol. Today **6:**270–275.
47. **Pang, G., A. Buret, E. O'Loughlin, A. Smith, R. Batey, and R. Clancy.** 1996. Immunologic, functional, and morphological characterization of three new human small intestinal epithelial cell lines. Gastroenterology **111:**8–18.
48. **Parenti, D. M.** 1989. Characterization of a thiol proteinase in Giardia lamblia. J. Infect. Dis. **160:**1076–1080.
49. **Samra, H. K., N. K. Ganguly, U. C. Garg, J. Goyal, and R. C. Mahajan.** 1988. Effect of excretory-secretory products of Giardia lamblia on glucose and phenylalanine transport in the small intestine of Swiss albino mice. Biochem. Int. **17:**801–812.
50. **Schmeiser, K., E. M. Hammond, S. Roberts, and R. J. Grand.** 1998. Specific cleavage of gamma catenin by caspases during apoptosis. FEBS Lett. **433:**51–57.
51. **Scott, K. G.-E., M. R. Logan, G. M. Klammer, D. A. Teoh, and A. G. Buret.** 2000. Jejunal brush border microvillous alterations in *Giardia muris*-infected mice: role of T lymphocytes and interleukin-6. Infect. Immun. **68:**3412–3418.
52. **Smith, P. D., F. D. Gillin, W. M. Spira, and T. E. Nash.** 1982. Chronic giardiasis: studies on drug sensitivity, toxin production, and host immune response. Gastroenterology **83:**797–803.
53. **Sun, Z., X. Wang, R. Wallen, X. Deng, X. Du, E. Hallberg, and R. Andersson.** 1998. The influence of apoptosis on intestinal barrier integrity in rats. Scand. J. Gastroenterol. **33:**415–422.
54. **Takano, J., and J. H. Yardley.** 1965. Jejunal lesions in patients with giardiasis and malabsorption: an electron microscopic study. Bull. Johns Hopkins Hosp. **116:**413–429.
55. **Teoh, D. A., D. Kamieniecki, G. Pang, and A. G. Buret.** 2000. Giardia lamblia rearranges F-actin and alpha-actinin in human colonic and duodenal monolayers and reduces transepithelial electrical resistance. J. Parasitol. **86:**800–806.
56. **Valenti, P., R. Greco, G. Pitari, P. Rossi, M. Ajello, G. Melino, and G. Antonini.** 1999. Apoptosis of Caco-2 intestinal cells invaded by Listeria monocytogenes: protective effect of lactoferrin. Exp. Cell Res. **250:**197–202.
57. **Widmann, C., S. Gibson, and G. L. Johnson.** 1998. Caspase-dependent cleavage of signaling proteins during apoptosis. A turn-off mechanism for anti-apoptotic signals. J. Biol. Chem. **273:**7141–7147.
58. **Youakim, A., and M. Ahdieh.** 1999. Interferon-gamma decreases barrier function in T84 cells by reducing ZO-1 levels and disrupting apical actin. Am. J. Physiol. **276:**G1279–G1288.

Editor: B. B. Finlay